



This is a repository copy of *White noise reduction for wideband linear array signal processing*.

White Rose Research Online URL for this paper:  
<http://eprints.whiterose.ac.uk/124737/>

Version: Accepted Version

---

**Article:**

Anbiyaei, M., Liu, W. [orcid.org/0000-0003-2968-2888](https://orcid.org/0000-0003-2968-2888) and McLernon, D. (2017) White noise reduction for wideband linear array signal processing. IET Signal Processing. ISSN 1751-9675

<https://doi.org/10.1049/iet-spr.2016.0730>

---

This paper is a postprint of a paper submitted to and accepted for publication in IET Signal Processing and is subject to Institution of Engineering and Technology Copyright. The copy of record is available at the IET Digital Library

**Reuse**

Unless indicated otherwise, fulltext items are protected by copyright with all rights reserved. The copyright exception in section 29 of the Copyright, Designs and Patents Act 1988 allows the making of a single copy solely for the purpose of non-commercial research or private study within the limits of fair dealing. The publisher or other rights-holder may allow further reproduction and re-use of this version - refer to the White Rose Research Online record for this item. Where records identify the publisher as the copyright holder, users can verify any specific terms of use on the publisher's website.

**Takedown**

If you consider content in White Rose Research Online to be in breach of UK law, please notify us by emailing [eprints@whiterose.ac.uk](mailto:eprints@whiterose.ac.uk) including the URL of the record and the reason for the withdrawal request.



[eprints@whiterose.ac.uk](mailto:eprints@whiterose.ac.uk)  
<https://eprints.whiterose.ac.uk/>

# White Noise Reduction for Wideband Linear Array Signal Processing

Mohammad Reza Anbiyaei<sup>†</sup>, Wei Liu<sup>†</sup> and Des C. McLernon<sup>\*</sup>

<sup>†</sup> Communications Research Group, Department of Electronic and Electrical Engineering, University of Sheffield,  
Sheffield S1 3JD, U.K.

<sup>\*</sup> Signal Processing for Communications Group, School of Electronic and Electrical Engineering,  
University of Leeds, Leeds LS2 9JT, U.K.

## Abstract

The performance of wideband array signal processing algorithms is dependent on the noise level in the system. A method is proposed for reducing the level of white noise in wideband linear arrays via a judiciously designed spatial transformation followed by a bank of highpass filters. A detailed analysis of the method and its effect on the spectrum of the signal and noise is presented. The reduced noise level leads to a higher signal to noise ratio (SNR) for the system, which can have a significant beneficial effect on the performance of various beamforming methods and other array signal processing applications such as direction of arrival (DOA) estimation. Here we focus on the beamforming problem and study the improved performance of two well-known beamformers, namely the reference signal based (RSB) and the linearly constrained minimum variance (LCMV) beamformers. Both theoretical analysis and simulation results are provided.

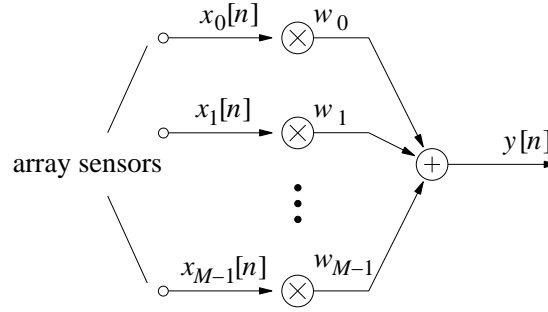
## Index Terms

White noise reduction, uniform linear arrays, nonuniform linear arrays, wideband beamforming, direction of arrival estimation, performance analysis.

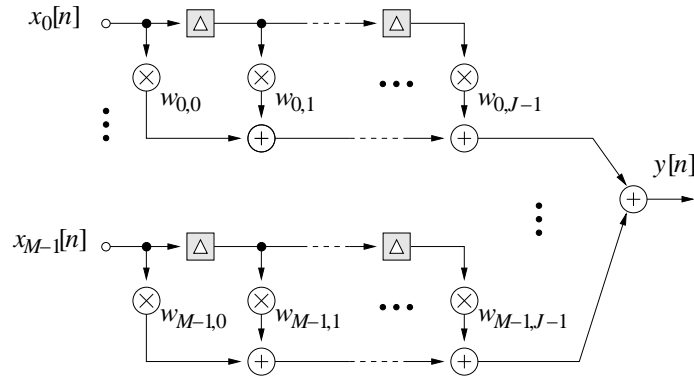
## I. INTRODUCTION

Wideband array signal processing, including beamforming and direction of arrival (DOA) estimation, has various applications in radar, sonar and wireless communications, and has been studied extensively in the past [1]–[9]. The performance of wideband array signal processing algorithms is dependent on the level of noise in the system, and normally the lower the level of noise, the better is the performance. Many methods have been developed in the past to reduce the noise level of a system, and one example is adaptive noise cancellation (ANC), which uses a reference undesired noise source and a primary source contaminated by noise, followed by adaptive filtering to produce a cleaned result [10], [11].

One common assumption for noise in wideband arrays is that it is both spatially (and in many cases also temporally) white. That is, the noise at one array sensor is uncorrelated with that at other sensors. Under this assumption, it seems that there is not much we can do about it and we have to simply accept whatever is left of the noise component after processing the signals. For example, in the simplest beamforming structure shown in Fig. 1a, the beamformer output  $y[n]$  is a linear combination of the received array signals  $x_0[n], x_1[n], \dots, x_{M-1}[n]$  weighted with the coefficients  $w_0, w_1, \dots, w_{M-1}$ . The values of these coefficients are obtained based on some criterion such as maximizing the output signal to interference plus noise ratio (SINR).



(a) A simple beamformer with its output  $y[n]$  given by a linear combination of the received array signals  $x_0[n]$ ,  $x_1[n]$ ,  $\dots$ ,  $x_{M-1}[n]$  weighted with the coefficients  $w_0$ ,  $w_1$ ,  $\dots$ ,  $w_{M-1}$ .



(b) A general wideband beamformer with  $M$  sensors and  $J$  taps.

Figure 1: General structure of narrowband and wideband beamformers

The question here is, whether there is anything that we can do to reduce the effect of white noise in a wideband array system (without attenuating the directional signals) so that the performance of the subsequent processing (such as DOA estimation and beamforming) could be improved.

In this paper, we aim to answer that question by developing a novel method to reduce the white noise level of a wideband array using a combination of a set of judiciously designed spatial transformations and a bank of filters, and the key is to realize that the white noise and the directional wideband signals received by the array have different spatial characteristics. Based on this difference, and motivated by the low-complexity subband-selective adaptive beamformer proposed in [12], we first transform the received wideband sensor signals into a new domain where the directional signals are decomposed in such a way that their corresponding outputs are associated with a series of tighter and tighter highpass spectra, while the spectrum of noise still covers the full band from  $-\pi$  to  $\pi$  in the normalized frequency domain. Then, a series of highpass filters with different cutoff frequencies are applied to selectively remove part of the noise spectrum while keeping the directional signals unchanged. Finally, an inverse transformation is applied to the filtered outputs to recover the original sensor signals, where compared to the original set of received sensor signals, the directional signals are left intact while the noise power has been reduced. The main assumption of the work is that the spectrum of the noise is white, and the noise between the sensors is uncorrelated. If the noise is correlated between the sensors, depending on the spectrum of the correlated noise and how the

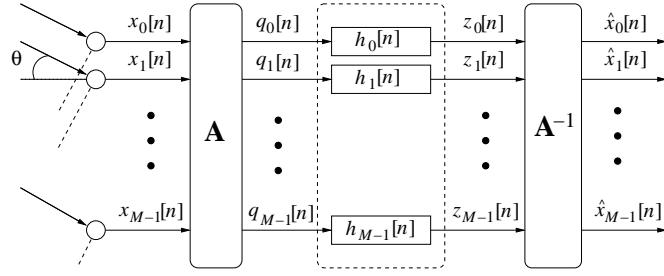


Figure 2: A block diagram for the general structure of the proposed noise reduction approach.

noise is correlated between the sensors, a different analysis would be needed.

Compared to our earlier published work in [13], where the idea was applied to uniform linear arrays (ULAs) for DOA estimation, in this paper, we extend it to arbitrary linear arrays and also focus on the beamforming problem. In particular, we give a detailed analysis of the spectrum of noise at different stages of the processing and provide theoretical results to show the improved performance; in addition, to accommodate the nonuniform linear array (NLA) geometry, a new design for the transformation matrix is proposed.

One condition placed on the transformation matrix is that it must be invertible. We have further assumed that it is also unitary and thus the discrete Fourier transform (DFT) matrix is used as a representative example for the ULA case and a least squares based design is introduced for the NLA case. Detailed analysis shows that the signal to noise ratio (SNR) of the array after the proposed processing can be improved by about 3dB in the ideal case. This is then translated into improved performance for beamforming, as demonstrated by both theoretical analysis and simulation results. Here we focus on two well-known beamformers, namely the reference signal based (RSB) [14]–[17], and the linearly constrained minimum variance (LCMV) beamformers [2], [18], [19].

This paper is organized as follows. In Section II, the general structure of our proposed method is first introduced. In Section III, the DFT matrix as a choice for the transformation matrix for ULAs is studied and the spectrum of noise at different stages of the processing is analysed. In Section IV, the adaptive beamformers and the effect of the noise reduction method on their correlation values are explained in detail. Extension of the method to the NLA case is provided In Section V. Simulation results based on the two adaptive beamformers are presented in Section VI in comparison with the theoretical results, and conclusions are drawn in Section VII.

## II. GENERAL STRUCTURE OF THE PROPOSED METHOD

Consider an  $M$ -element arbitrary linear array. A block diagram for the general structure of the proposed method is shown in Fig. 2. The  $M$  received array signals  $x_m[n]$ ,  $m = 0, \dots, M-1$ , are first processed by an  $M \times M$  transformation matrix  $\mathbf{A}$ , and then its outputs  $q_m[n]$ ,  $m = 0, \dots, M-1$ , pass through a bank of highpass filters with impulse responses given by  $h_m[n]$ ,  $m = 0, \dots, M-1$ . The outputs of these filters are denoted by  $z_m[n]$ ,  $m = 0, \dots, M-1$  and these are then transformed by the  $M \times M$  inverse transformation  $\mathbf{A}^{-1}$ . For simplicity we assume  $\mathbf{A}$  is unitary, i.e.,  $\mathbf{A}^{-1} = \mathbf{A}^H$ , where  $\{\cdot\}^H$  denotes Hermitian transpose.

There are two components for the received array signal  $x_m[n]$  at the  $m$ -th sensor: the signal part  $s_m[n]$  and the white noise part  $b_m[n]$ . So we have:

$$x_m[n] = s_m[n] + b_m[n]. \quad (1)$$

The total signal vector  $\mathbf{x}[n]$  can be expressed as

$$\mathbf{x}[n] = \mathbf{s}[n] + \mathbf{b}[n], \quad (2)$$

where

$$\begin{aligned} \mathbf{x}[n] &= [x_0[n], x_1[n], \dots, x_{M-1}[n]]^T, \\ \mathbf{s}[n] &= [s_0[n], s_1[n], \dots, s_{M-1}[n]]^T, \\ \mathbf{b}[n] &= [b_0[n], b_1[n], \dots, b_{M-1}[n]]^T. \end{aligned}$$

Applying the  $M \times M$  transformation matrix  $\mathbf{A}$  to the signal vector  $\mathbf{x}[n]$ , we obtain the output signal vector  $\mathbf{q}[n]$  as

$$\mathbf{q}[n] = \mathbf{A}\mathbf{x}[n], \quad (3)$$

where

$$\mathbf{q}[n] = [q_0[n], q_1[n], \dots, q_{M-1}[n]]^T.$$

The element of  $\mathbf{A}$  at the  $m$ -th row and  $l$ -th column is denoted by  $a_{m,l}$ , i.e.,  $[\mathbf{A}]_{m,l} = a_{m,l}$ . Each row vector of  $\mathbf{A}$  acts as a simple beamformer, and its output  $q_m[n]$  is given by

$$q_m[n] = \sum_{l=0}^{M-1} a_{m,l} x_l[n]. \quad (4)$$

The beam response  $R_m(\Omega, \theta)$  of this simple beamformer as a function of the normalized frequency  $\Omega$  and the DOA angle  $\theta$  is [12], [20],

$$R_m(\Omega, \theta) = \sum_{l=0}^{M-1} a_{m,l} e^{-i\mu_l \Omega \sin \theta}, \quad (5)$$

where  $\mu_l = d_l/cT_s$  and  $\Omega = \omega T_s$ , with  $d_l$  being the distance from the zero-th sensor to the  $l$ -th sensor (where  $d_0=0$ ),  $c$  the wave propagation speed,  $T_s$  the sampling period, and  $\omega$  the angular frequency of signals.

With  $\hat{\Omega} = \Omega \sin \theta$ , we can obtain an alternative representation of  $R_m(\Omega, \theta)$  as follows

$$A_m(\hat{\Omega}) = \sum_{l=0}^{M-1} a_{m,l} e^{-i\mu_l \hat{\Omega}}, \quad (6)$$

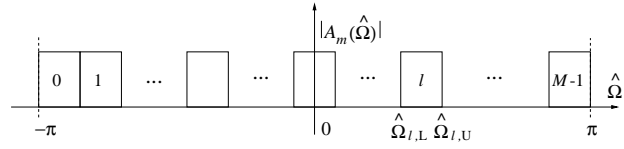
where  $\hat{\Omega}$  is representing the spatial frequency of the received signal,  $A_m(\hat{\Omega})$  is the frequency response of the  $m$ -th row vector of the  $M \times M$  transformation matrix  $\mathbf{A}$  (if we consider each row vector as the impulse response of a finite impulse response (FIR) filter).

Similar to [12], the frequency responses  $A_m(\hat{\Omega})$ ,  $m = 0, 1, \dots, M-1$ , are arranged to be bandpass, each with a bandwidth  $2\pi/M$ . The row vectors of  $\mathbf{A}$  all together cover the whole frequency band which is  $[-\pi : \pi]$ . An ideal example for an odd number  $M$  is shown in Fig. 3a.

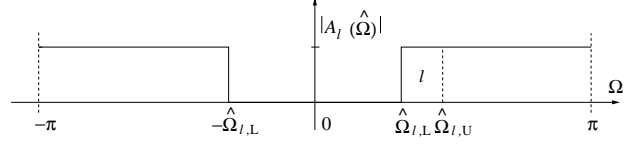
The bandpass filters, which are used as row vectors of  $\mathbf{A}$ , have a highpass filtering effect on the received array signals. To examine this highpass behaviour, the  $l$ -th row vector is analyzed. The frequency response of this row vector is shown in Fig. 3a, which is:

$$|A_l(\hat{\Omega})| = \begin{cases} 1, & \text{for } \hat{\Omega} \in [\hat{\Omega}_{l,L} : \hat{\Omega}_{l,U}] \\ 0, & \text{otherwise.} \end{cases} \quad (7)$$

As  $\sin \theta \in [-1 : 1]$  when  $\theta \in [-\pi/2 : \pi/2]$ , the possible maximum frequency component of the  $l$ -th row vector  $A_l(\hat{\Omega})$  is  $\Omega = \pi$ , which corresponds to  $|\sin \theta| = \hat{\Omega}_{l,U}/\pi$  when  $\hat{\Omega}_{l,L} \geq 0$ , while the minimum frequency component is  $\Omega = \hat{\Omega}_{l,L}$ , which corresponds to  $|\sin \theta| = 1$ , then we have the response of  $A_l(\Omega \sin \theta)$  as a function of  $\Omega$  in the following:



(a) Frequency responses of the row vectors of  $\mathbf{A}$  in the ideal case for an odd number  $M$ .



(b) The highpass filtering effect of the  $l$ -th row vector in the ideal case.

Figure 3: Frequency responses of the row vectors of  $\mathbf{A}$  in the ideal case and the highpass filtering effect of a sample row vector.

$$|A_l(\Omega \sin \theta)| = \begin{cases} 1, & \text{for } \Omega \in [\hat{\Omega}_{l,L} : \pi] \\ 0, & \text{otherwise.} \end{cases} \quad (8)$$

as shown in Fig. 3b.

Considering the above frequency response, the received array signal components with frequency of  $\Omega \in [-\hat{\Omega}_{l,L} : \hat{\Omega}_{l,L}]$  will not “pass” through this row vector, since  $\hat{\Omega} = \Omega \sin \theta$  does not fall into the passband of  $[\hat{\Omega}_{l,L} : \hat{\Omega}_{l,U}]$ , no matter what value the DOA angle  $\theta$  takes. Therefore, the frequency range of the output is  $|\Omega| \geq \hat{\Omega}_{l,L}$  and the lower bound is determined by  $\hat{\Omega}_{l,L}$  when  $\hat{\Omega}_{l,L} > 0$ . Alternatively, the lower bound is determined by  $|\hat{\Omega}_{l,U}|$  when  $\hat{\Omega}_{l,L} < \hat{\Omega}_{l,U} < 0$ .

As a result, the output spectrum of the directional signal part of  $q_l[n]$  corresponding to the  $l$ -th row vector will then be highpass filtered as shown in Fig. 3b. As the noise part in  $\mathbf{x}[n]$  is spatially white, the output noise spectrum of the row vector is still a constant, covering the whole spectrum. As shown in Fig. 2, the output  $q_l[n]$  of each row vector is the input to a corresponding highpass filter  $h_l[n]$ ,  $l = 0, 1, \dots, M-1$ . These highpass filters should cover the whole bandwidth of the signal part of the output  $q_l[n]$  and therefore have the same frequency response as specified in Fig. 3b. As a result, in the ideal case, the highpass filters will not have any effect on the signal components and all the signal components will pass through the highpass filters without any distortion. But then the frequency components of the white noise falling into the stopband of these highpass filters will be removed.

The output of the highpass filters is the convolution of each row vector output and its corresponding highpass filter,

$$\mathbf{z}[n] = \begin{bmatrix} z_0[n] \\ \vdots \\ z_{M-1}[n] \end{bmatrix} = \begin{bmatrix} q_0[n] * h_0[n] \\ \vdots \\ q_{M-1}[n] * h_{M-1}[n] \end{bmatrix}, \quad (9)$$

where  $*$  denotes the convolution operator.

Now we consider the noise reduction effect of these filters. Each filter removes part of the noise except for that part corresponding to the row vector with a frequency response covering the zero frequency component, which should allow all frequencies to pass. Assume now that the size  $M$  of the array is an odd number. From Fig. 3, for the first row vector  $A_0(\hat{\Omega})$ ,  $2/M$  part of the noise passes, while for  $A_l(\hat{\Omega})$ ,  $4/M$  part of the noise passes, and so on. For the row vector with frequency

response covering the zero frequency, all of the noise will pass. For the row vectors with frequency responses larger than the zero frequency, the highpass filtering is a replica of the bands with frequency responses lower than the zero frequency. Therefore, in the ideal case, the ratio between the total noise power after and before the processing of the  $M$  highpass filters can be expressed as

$$\frac{P_{bo}}{P_{bi}} = \frac{1}{M} \left( 1 + 2 \left( \frac{2}{M} + \frac{4}{M} + \dots + \frac{M-1}{M} \right) \right), \quad (10)$$

where  $P_{bo}$  is the total noise power at the output of the filters and  $P_{bi}$  is the total noise power at their input. Following the same procedure, if the size of the array is an even number, then this ratio is given by

$$\frac{P_{bo}}{P_{bi}} = \frac{1}{M} \left( 1 + 2 \left( \frac{3}{M} + \frac{5}{M} + \dots + \frac{M-1}{M} \right) + \frac{1}{M} \right). \quad (11)$$

As a result, we have

$$r(M) = \frac{P_{bo}}{P_{bi}} = \begin{cases} \frac{M^2+2M-1}{2M^2}, & \text{if } M \geq 1 \text{ is odd} \\ \frac{M^2+2M-2}{2M^2}, & \text{if } M \geq 2 \text{ is even.} \end{cases} \quad (12)$$

When  $M \rightarrow \infty$ , noise power will be reduced by half in both cases. Since the highpass filters have no effect on the signal part, the ratio between the total signal power and the total noise power will be improved by almost 3dB in the ideal case. For a finite  $M$ , the improvement will be less than 3dB. For example, when  $M = 16$ , it is about 2.53dB.

Applying the inverse of the transformation matrix  $\mathbf{A}^{-1} = \mathbf{A}^H$  (with size  $M \times M$ ) to  $\mathbf{z}[n]$ , we obtain the estimates of the original input sensor signals  $\hat{x}_m[n]$ ,  $m = 0, 1, \dots, M-1$ . In vector form, we have

$$\hat{\mathbf{x}}[n] = \mathbf{A}^{-1} \mathbf{z}[n], \quad (13)$$

where  $\hat{\mathbf{x}}[n] = [\hat{x}_0[n], \hat{x}_1[n], \dots, \hat{x}_{M-1}[n]]^T$ .

After going through these processing stages, there is no change in the signal part at the final output  $\hat{x}_l[n]$ ,  $l = 0, 1, \dots, M-1$  compared to the original signal part in  $x_l[n]$ ,  $l = 0, 1, \dots, M-1$ . On the contrary, since  $\mathbf{A}^{-1}$  is also unitary, the total noise power stays the same between  $\hat{\mathbf{x}}[n]$  and  $\mathbf{z}[n]$ , which is almost half the total noise power in  $\mathbf{x}[n]$ . Therefore, for a very large array size  $M$ , we have

$$\|\hat{\mathbf{x}}[n]\|_2^2 \approx \|\mathbf{s}[n]\|_2^2 + \frac{1}{2} \|\mathbf{b}[n]\|_2^2. \quad (14)$$

where  $\|\cdot\|_2$  is the  $l_2$  norm.

Based on above discussion, in terms of the total signal power to total noise power ratio (TSNR), we have the following relationship

$$TSNR_{\hat{\mathbf{x}}} \approx \frac{\|\mathbf{s}[n]\|_2^2}{\frac{1}{2} \|\mathbf{b}[n]\|_2^2} = 2TSNR_{\mathbf{x}}. \quad (15)$$

So in the ideal case, for a very large  $M$ , the TSNR is almost doubled by the proposed noise reduction method. This can be translated into better performance for different array processing applications such as beamforming and DOA estimation. In the following section, using the DFT-based transformation matrix for ULAs, we analyse the theoretical result for two commonly used beamformers to show the performance improvement in the ideal case.

### III. ANALYSIS BASED ON THE DFT MATRIX FOR ULAS

The transformation matrix is the most important part of the system. It should have a full rank so that an inverse transform can be applied at the end to recover the signals. Another key requirement is to make sure its row vectors have the desired bandpass frequency responses shown in Fig. 3a. So, in general the design of the transformation matrix can be formulated as

a constrained FIR filter design problem. This is similar to the beamspace transformation problem studied in [21]–[23], and as pointed out there, we could design a prototype lowpass filter and then modulate it to different frequency bands by a DFT operation or use the DFT matrix directly. In particular, the DFT matrix is unitary, which will simplify our theoretical analysis and provide us with the crucial insight into the performance of the proposed structure.

Using the DFT matrix for an  $M \times M$  transformation  $\mathbf{A}$ , with  $\gamma = e^{-i(2\pi/M)}$ , we have

$$\mathbf{A} = \frac{1}{\sqrt{M}} \begin{bmatrix} \gamma^{0 \cdot 0} & \gamma^{0 \cdot 1} & \dots & \gamma^{0 \cdot (M-1)} \\ \gamma^{1 \cdot 0} & \gamma^{1 \cdot 1} & \dots & \gamma^{1 \cdot (M-1)} \\ \vdots & \vdots & \ddots & \vdots \\ \gamma^{(M-1) \cdot 0} & \gamma^{(M-1) \cdot 1} & \dots & \gamma^{(M-1) \cdot (M-1)} \end{bmatrix}. \quad (16)$$

Next, an analysis of the signal spectrum based on such a transformation matrix at different stages of the proposed structure is provided.

#### A. Spectrum Analysis with DFT Matrix

Now we study the input-output relationships in the frequency domain based on the DFT matrix. We first have

$$\hat{\mathbf{x}}(\Omega) = \mathbf{A}^{-1} \mathbf{H} \mathbf{A} \mathbf{x}(\Omega), \quad (17)$$

where  $\hat{\mathbf{x}}(\Omega)$  and  $\mathbf{x}(\Omega)$  are the vectors holding the discrete-time Fourier transforms (DTFTs) of the time-domain signal vectors  $\hat{\mathbf{x}}[n]$  and  $\mathbf{x}[n]$ , respectively, and  $\mathbf{H}$  is an  $M \times M$  real valued diagonal matrix with its diagonal elements being the frequency responses  $H_m(\Omega)$  of the corresponding filters  $h_m[n]$ ,  $m = 0, 1, \dots, M-1$ , i.e.,

$$\mathbf{H} = \begin{bmatrix} H_0(\Omega) & 0 & \dots & 0 \\ 0 & H_1(\Omega) & \dots & 0 \\ \vdots & \vdots & \ddots & \vdots \\ 0 & 0 & \dots & H_{M-1}(\Omega) \end{bmatrix}. \quad (18)$$

From (17), the transfer function of the system is:

$$\mathbf{T} = \mathbf{A}^{-1} \mathbf{H} \mathbf{A} = \mathbf{A}^{-1} \frac{1}{\sqrt{M}} \begin{bmatrix} H_0 \gamma^{0 \cdot 0} & \dots & H_0 \gamma^{0 \cdot (M-1)} \\ H_1 \gamma^{1 \cdot 0} & \dots & H_1 \gamma^{1 \cdot (M-1)} \\ \vdots & \ddots & \vdots \\ H_{M-1} \gamma^{(M-1) \cdot 0} & \dots & H_{M-1} \gamma^{(M-1) \cdot (M-1)} \end{bmatrix}. \quad (19)$$

Then, all the elements of  $\mathbf{T}$  (complex valued, with size  $M \times M$ ) can be obtained. Considering the relationship between the terms, we can derive a general form for the elements of  $\mathbf{T}$  and the element at the  $u$ -th row and  $v$ -th column is given by

$$T_{u,v} = \frac{1}{M} \sum_{l=0}^{M-1} H_l \gamma^{-lu} \gamma^{lv} = \frac{1}{M} \sum_{l=0}^{M-1} H_l \gamma^{l(v-u)}. \quad (20)$$

So we have

$$\hat{\mathbf{x}}(\Omega) = \mathbf{T} \mathbf{x}(\Omega). \quad (21)$$

We are interested in the spectrum of the noise at the output. The relationship between the input and output signals' spectrum is [24],

$$\mathbf{S}_{\hat{\mathbf{x}}}(\Omega) = \mathbf{T} \mathbf{T}^*(\Omega) \mathbf{S}_{\mathbf{x}}(\Omega). \quad (22)$$



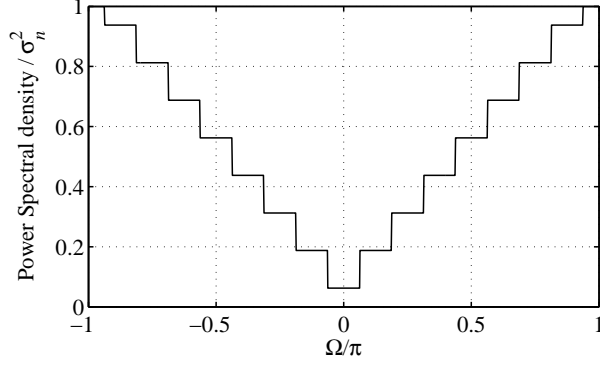


Figure 4: Power spectrum of the output of the noise reduction system with  $M=16$ .

$\mathbf{S}_{\hat{\mathbf{x}}}(\Omega)$  and  $\mathbf{S}_{\mathbf{x}}(\Omega)$  are  $M \times M$  matrices, where each matrix element represents the cross-spectral density of the two corresponding signals.  $\mathbf{S}_{\mathbf{x}}(u, v)$  is the  $(u, v)$ -th element of  $\mathbf{S}_{\mathbf{x}}$  and it is the cross-spectral density between  $x_u[n]$  and  $x_v[n]$ . It can be easily proved that the cross spectral density is equal to the DTFT of the cross correlation function of the two signals [25]. Then we have

$$\mathbf{S}_{\mathbf{x}}(u, v) = x_u^*(\Omega)x_v(\Omega), \quad (23)$$

where the asterisk denotes the complex conjugate. Similarly, we have  $\mathbf{S}_{\hat{\mathbf{x}}}(u, v) = \hat{x}_u^*(\Omega)\hat{x}_v(\Omega)$ .

Now we consider the noise part. The spectral density of the white noise is  $\sigma_b^2$ , where  $\sigma_b^2$  is the variance of the noise. Since the noise received by each array sensor is uncorrelated, the noise spectral density of a sensor is  $\mathbf{S}_{\mathbf{b}}(u, u) = \sigma_b^2$  and the noise cross spectral density between two sensors is  $\mathbf{S}_{\mathbf{b}}(u, v) = 0$ . So, the spectrum of the noise received by the array is:

$$\mathbf{S}_{\mathbf{b}}(\Omega) = \sigma_b^2 \begin{bmatrix} 1 & 0 & \cdots & 0 \\ 0 & 1 & \cdots & 0 \\ \vdots & \vdots & \ddots & \vdots \\ 0 & 0 & \cdots & 1 \end{bmatrix} = \sigma_b^2 \mathbf{I}, \quad (24)$$

where  $\mathbf{I}$  is the  $M \times M$  identity matrix. Therefore, (22) can be written as

$$\mathbf{S}_{\hat{\mathbf{b}}}(\Omega) = \mathbf{T}\mathbf{T}^*(\Omega)\sigma_b^2\mathbf{I}. \quad (25)$$

$\mathbf{S}_{\hat{\mathbf{b}}}(\Omega)$  is an  $M \times M$  complex valued matrix with real values on the diagonal. Each term of  $\mathbf{S}_{\hat{\mathbf{b}}}(\Omega)$  is given by:

$$\mathbf{S}_{\hat{\mathbf{b}}}(u, v)(\Omega) = \frac{\sigma_b^2}{M} \sum_{l=0}^{M-1} T_{u,l}T_{v,l}^*. \quad (26)$$

From (20) and (26), we have:

$$\mathbf{S}_{\hat{\mathbf{b}}}(u, v)(\Omega) = \frac{\sigma_b^2}{M} \sum_{l=0}^{M-1} H_l(\Omega)e^{i\frac{2\pi}{M}(u-v)l}. \quad (27)$$

The spectrum of the noise for  $M = 16$  is shown in Fig. 4 in the ideal case. The next step is to take the inverse DTFT from (27) to calculate the correlation function in the time domain. The inverse Fourier transform of (27) is:

$$\begin{aligned} R_{\hat{\mathbf{b}}(u,v)}(\tau) &= \text{DTFT}^{-1} \left\{ \frac{\sigma_b^2}{M} \sum_{l=0}^{M-1} H_l(\Omega)e^{i\frac{2\pi}{M}(u-v)l} \right\} \\ &= \frac{\sigma_b^2}{M} \sum_{l=0}^{M-1} e^{i\frac{2\pi}{M}(u-v)l} \text{DTFT}^{-1} \{H_l(\Omega)\}. \end{aligned} \quad (28)$$

where  $\tau$  is an arbitrary delay and  $R_{\hat{b}(u,v)}(\tau)$  is the correlation function between the filtered noise at the  $u$ -th and the  $v$ -th array elements after applying the noise reduction method. As the only term which is a function of frequency is  $H_l(\Omega)$ , the inverse DTFT only applies to this part. The frequency response of a single highpass filter has the same form as that shown in Fig. 3b. To calculate  $\text{DTFT}^{-1}\{H_l(\Omega)\}$ , (28) can be written as

$$R_{\hat{b}(u,v)}(\tau) = \frac{\sigma_b^2}{M} \sum_{l=0}^{M-1} \frac{\pi - \hat{\Omega}_{l,L}}{\pi} e^{j\frac{2\pi}{M}(u-v)l} e^{j\frac{\pi + \hat{\Omega}_{l,L}}{2}\tau} \text{sinc}\left(\frac{\pi - \hat{\Omega}_{l,L}}{2}\tau\right), \quad (29)$$

where  $\pi$  is the maximum normalized frequency and  $\hat{\Omega}_{l,L}$  is the lower bound frequency of the  $l$ -th highpass filter as was previously shown in Fig. 3b. The correlation values regarding different time delays can be calculated from (28) and will be used when we derive the theoretical performance results for different wideband beamformers.

#### IV. PERFORMANCE ANALYSIS OF THE PROPOSED METHOD FOR ADAPTIVE WIDEBAND BEAMFORMING

For wideband beamforming, a tapped delay-line (TDL) is normally employed, with Fig. 1b showing a general structure. The TDL has a length of  $J$  and the coefficient for the  $m$ -th sensor at the  $j$ -th position of the TDL is denoted by  $w_{m,j}$ . All  $J$  weights at the  $m$ -th TDL form an *element* weight vector  $\mathbf{w}_m$  and all  $M$  element weight vectors form a  $MJ \times 1$  *total* weight vector  $\mathbf{w}$ , where

$$\mathbf{w}_m = [w_{m,0}, w_{m,1}, \dots, w_{m,J-1}]^T, \quad (30)$$

$$\mathbf{w} = [\mathbf{w}_0^T, \mathbf{w}_1^T, \dots, \mathbf{w}_{M-1}^T]^T. \quad (31)$$

The beamformer output  $y[n]$  is given by

$$y[n] = \mathbf{w}^T \mathbf{x}, \quad (32)$$

where the input signal vector  $\mathbf{x}$  is defined as

$$\mathbf{x} = [\mathbf{x}^T[n], \mathbf{x}^T[n-1], \dots, \mathbf{x}^T[n-J+1]]^T \quad (33)$$

$$\mathbf{x}[n-j] = [x_0[n-j], x_1[n-j], \dots, x_{M-1}[n-j]]^T. \quad (34)$$

The idea is to process the received array signal by the noise reduction method, so that the noise level in received signal will be reduced; then, the recovered array signals with reduced noise level will be fed to the following beamformers. In the following, two widely-used adaptive beamforming methods are briefly reviewed and the theoretical performance results are then derived based on the proposed noise reduction method.

##### A. Reference Signal Based Adaptive Beamformer

The reference signal based (RSB) beamformer is normally employed when a reference signal  $r[n]$  is available, where the weight vector of the beamformer can be adjusted to minimize the mean square error (MSE) between the reference signal and the beamformer output  $y[n]$  [14], [15], [17], [26]. The  $MJ \times 1$  optimal weight vector is given by:

$$\mathbf{w}_{opt} = \Phi_x^{-1} \mathbf{s}_d, \quad (35)$$

where  $\Phi_x$  is the signal correlation matrix with size  $MJ \times MJ$ ,

$$\Phi_x = E[\mathbf{x}^* \mathbf{x}^T], \quad (36)$$

( $E\{\cdot\}$  denotes the statistical expectation) and  $\mathbf{s}_d$  is the reference correlation vector with size  $MJ \times 1$ ,

$$\mathbf{s}_d = E[\mathbf{x}^* r_0[n]], \quad (37)$$

with  $r_0[n]$  being the normalized reference signal with unit power.

There are three components for each of the received sensor signals: desired signal, interference and noise. So, the signal vector  $\mathbf{x}$  can be decomposed into three corresponding parts:

$$\mathbf{x} = \mathbf{x}_d + \mathbf{x}_i + \mathbf{x}_b. \quad (38)$$

Since the desired signal, interference and noise are uncorrelated with each other,  $\Phi_{\mathbf{x}}$  can be decomposed into three  $MJ \times MJ$  correlation matrices corresponding to the desired signal, interference and white noise components, respectively. i.e.,

$$\Phi_{\mathbf{x}} = \Phi_d + \Phi_i + \Phi_b. \quad (39)$$

Assuming the reference signal is the same as the desired signal,  $\mathbf{s}_d$  in (37) can be simplified to

$$\mathbf{s}_d = E[\mathbf{x}^* r_0[n]] = E[\mathbf{x}_d^* r_0[n]]. \quad (40)$$

More details for calculating  $\mathbf{w}_{opt}$  from (35) can be found in [15].

For our proposed noise reduction method, in the ideal case the directional signals (desired and interference) remain intact and only the noise part is reduced/changed. Then, the total signal vector  $\hat{\mathbf{x}}$  corresponding to  $\mathbf{x}$  after noise reduction can be expressed as:

$$\hat{\mathbf{x}} = \mathbf{x}_d + \mathbf{x}_i + \hat{\mathbf{x}}_b. \quad (41)$$

where  $\hat{\mathbf{x}}_b$  is the part of  $\hat{\mathbf{x}}$  corresponding to the reduced noise after the proposed processing.

Similarly the correlation matrices  $\Phi_d$  and  $\Phi_i$  will remain the same after noise reduction, but the correlation matrix for the noise part will be changed to  $\Phi_{\hat{b}}$  with size  $MJ \times MJ$ . Then, the  $MJ \times MJ$  correlation matrix  $\Phi_{\hat{\mathbf{x}}}$  after noise reduction can be expressed as:

$$\Phi_{\hat{\mathbf{x}}} = \Phi_d + \Phi_i + \Phi_{\hat{b}}. \quad (42)$$

We can obtain  $\Phi_{\hat{b}}$  from (28) and partition it into  $M \times M$  submatrices (each submatrix is  $J \times J$ ),

$$\Phi_{\hat{b}} = \begin{bmatrix} \Phi_{\hat{b}_{0,0}} & \cdots & \Phi_{\hat{b}_{0,M-1}} \\ \vdots & \ddots & \vdots \\ \Phi_{\hat{b}_{M-1,0}} & \cdots & \Phi_{\hat{b}_{M-1,M-1}} \end{bmatrix}. \quad (43)$$

where  $\Phi_{\hat{b}_{u,v}} = E[\hat{\mathbf{x}}_{b_u}^* \hat{\mathbf{x}}_{b_v}^T]$ . The delay between two adjacent taps in a TDL is  $T_0 = \frac{\pi r}{2\Omega_0}$ , where  $\Omega_0$  is the centre frequency and  $r$  is the number of quarter-wave delays in  $T_0$  at frequency  $\Omega_0$ . Hence the delay between the  $j$ -th and  $k$ -th tap is  $\tau = (j-k)T_0$ . Therefore the correlation value  $[\Phi_{\hat{b}_{u,v}}]_{j,k}$  between the noise (after the proposed processing) at the  $j$ -th tap of the  $u$ -th element and that at the  $k$ -th tap of the  $v$ -th element is given by

$$[\Phi_{\hat{b}_{u,v}}]_{j,k} = E[b_{u,j}^*[n] b_{v,k}[n]] = R_{b(u,v)}[(j-k)T_0]. \quad (44)$$

With the result in (29), we have

$$[\Phi_{\hat{b}_{u,v}}]_{j,k} = \frac{\sigma_b^2}{M} \sum_{l=0}^{M-1} \frac{\pi - \hat{\Omega}_{l,L}}{\pi} e^{i \frac{2\pi}{M} (u-v)l} e^{i \frac{\pi + \hat{\Omega}_{l,L}}{2} (j-k)T_0} \times \text{sinc}\left(\frac{\pi - \hat{\Omega}_{l,L}}{2} (j-k)T_0\right). \quad (45)$$

Now we have all the correlation values required for calculating the  $\mathbf{w}_{opt}$  in (35) and the beamformer output  $y[n]$  is

$$y[n] = \mathbf{w}_{opt}^T \hat{\mathbf{x}}, \quad (46)$$

with its power given by

$$P = \frac{1}{2}E[\|y[n]\|^2] = \frac{1}{2}\mathbf{w}_{opt}^H \mathbf{\Phi}_{\hat{\mathbf{x}}} \mathbf{w}_{opt}; \quad (47)$$

The output SINR is given by

$$SINR = \frac{P_d}{P_i + P_b} \quad (48)$$

where

$$P_d = \mathbf{w}_{opt}^H \mathbf{\Phi}_d \mathbf{w}_{opt} \quad (49)$$

$$P_i = \mathbf{w}_{opt}^H \mathbf{\Phi}_i \mathbf{w}_{opt} \quad (50)$$

$$P_b = \mathbf{w}_{opt}^H \mathbf{\Phi}_b \mathbf{w}_{opt}. \quad (51)$$

### B. Linearly Constrained Minimum Variance Beamformer

In practice, the reference signal assumed in Section IV-A may be unavailable. However, when some information on the DOAs as well as the bandwidth limits of the desired signal and/or the interferences is available, a linearly constrained minimum variance (LCMV) beamformer can be employed for effective beamforming [2], [27]. The LCMV beamformer is formulated as follows (based on the recovered signal  $\hat{\mathbf{x}}$  after the proposed noise reduction method),

$$\min_{\mathbf{w}} \mathbf{w}^H \mathbf{\Phi}_{\hat{\mathbf{x}}} \mathbf{w} \quad \text{subject to} \quad \mathbf{C}^H \mathbf{w} = \mathbf{f}, \quad (52)$$

where  $\mathbf{w}$  and  $\mathbf{\Phi}_{\hat{\mathbf{x}}}$  are defined as before in Section IV-A,  $\mathbf{C}$  is the  $MJ \times J$  constraint matrix and  $\mathbf{f}$  is the  $J \times 1$  response vector. The solution to (52) can be obtained using the Lagrange multipliers method,

$$\mathbf{w}_{opt} = \mathbf{\Phi}_{\hat{\mathbf{x}}}^{-1} \mathbf{C} (\mathbf{C}^H \mathbf{\Phi}_{\hat{\mathbf{x}}}^{-1} \mathbf{C})^{-1} \mathbf{f}. \quad (53)$$

Suppose the desired signal comes from the broadside, i.e.,  $\theta_d = 0^\circ$ . Then,  $\mathbf{C}$  and  $\mathbf{f}$  have a very simple form [2]. With the optimal weight vector determined, the output SINR can be obtained as in Section IV-A.

## V. EXTENSION OF THE NOISE REDUCTION METHOD FOR NLAS

As an example for a unitary matrix with a good bandpass response, we have considered the DFT matrix in the ULA case. However, the DFT matrix is not applicable for the NLA case, since it does not have a uniform spacing, and the resultant beams by each row vector of such a transformation will be significantly distorted.

Therefore, we use a different approach for designing the transformation matrix for NLAs by introducing a least squares based design method here. The idea is to use an ideal unitary beam response such as those of a DFT matrix as the reference response for the least squares method to design a prototype filter  $\mathbf{p}$  (where  $[\mathbf{p}]_l = p_l, l = 0, \dots, M-1$ ), and then we modulate it into different subbands in a uniform way to form the required transformation matrix.

The least squares filter design method has been well studied in the past [2], [28]. Given the desired beam pattern  $P_d(\hat{\Omega})$  and considering  $\mathbf{d}(\hat{\Omega})$  as the steering vector of the NLA,

$$\mathbf{d}(\hat{\Omega}) = \begin{bmatrix} 1 & e^{-i\frac{d_1}{cT_s}\hat{\Omega}} & \dots & e^{-i\frac{d_{M-1}}{cT_s}\hat{\Omega}} \end{bmatrix}, \quad (54)$$

the problem can be solved by minimizing the sum of squares of the error between  $P_d(\hat{\Omega})$  and the designed response  $P(\hat{\Omega})$  over the frequency range of interest, i.e.,

$$\min_{\mathbf{p}} \sum_{\hat{\Omega}_{pb}} |P(\hat{\Omega}) - P_d(\hat{\Omega})|^2, \quad (55)$$

Minimizing the above cost function with respect to the coefficients vector  $\mathbf{p}$  gives the standard least squares solution,

$$\mathbf{p}_{opt} = \mathbf{G}_{ls}^{-1} \mathbf{g}_{ls}, \quad (56)$$

with

$$\mathbf{G}_{ls} = \sum_{\hat{\Omega}_{pb}} \mathbf{d}(\hat{\Omega}) \mathbf{d}^H(\hat{\Omega}),$$

$$\mathbf{g}_{ls} = \sum_{\hat{\Omega}_{pb}} (\mathbf{d}_R(\hat{\Omega}) P_{d,R}(\hat{\Omega}) + \mathbf{d}_I(\hat{\Omega}) P_{d,I}(\hat{\Omega})),$$

where  $\mathbf{d}_R(\hat{\Omega})$  and  $P_{d,R}(\hat{\Omega})$  denote the real parts of  $\mathbf{d}(\hat{\Omega})$  and  $P_d(\hat{\Omega})$ , and  $\mathbf{d}_I(\hat{\Omega})$  and  $P_{d,I}(\hat{\Omega})$  are their imaginary parts.

Then, we modulate  $\mathbf{p}$  to cover the whole normalized frequency band,

$$A_{m,l} = e^{-i \frac{2\pi}{M} m \frac{d_l}{cT_s}} p_l, \quad (57)$$

where  $m = 0, \dots, M-1$ ,  $l = 0, \dots, M-1$ .

At this stage if the condition number of the resultant transformation matrix is high, we can use the diagonal loading method [29] to reduce the condition number,

$$\mathbf{A}_L = \mathbf{A} + \alpha \mathbf{I}, \quad (58)$$

where  $\alpha$  is a constant representing a small loading level.

Note that the transformation matrix obtained by the above procedure will not be unitary in general and how to design a unitary matrix for NLAs with the required bandpass filtering effect is still an open problem for our future research. However, we will see in the simulations part that the transformation matrix obtained from the above procedure works well to some degree and provides a clear performance improvement.

## VI. SIMULATION RESULTS

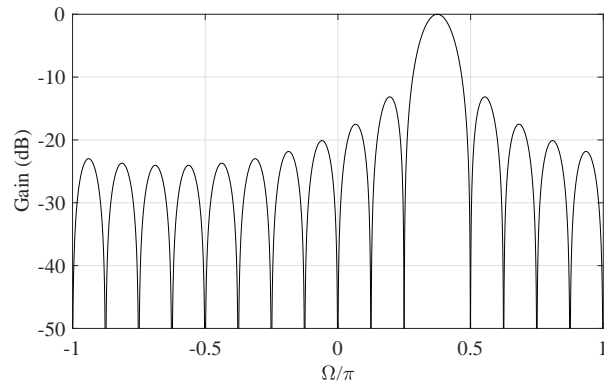
In this section, simulation results will be provided for both ULAs and NLAs, and the performance improvement by the proposed noise reduction (NR) method for RSB and LCMV beamformers will be examined.

### A. Performance of the NR Method for ULA

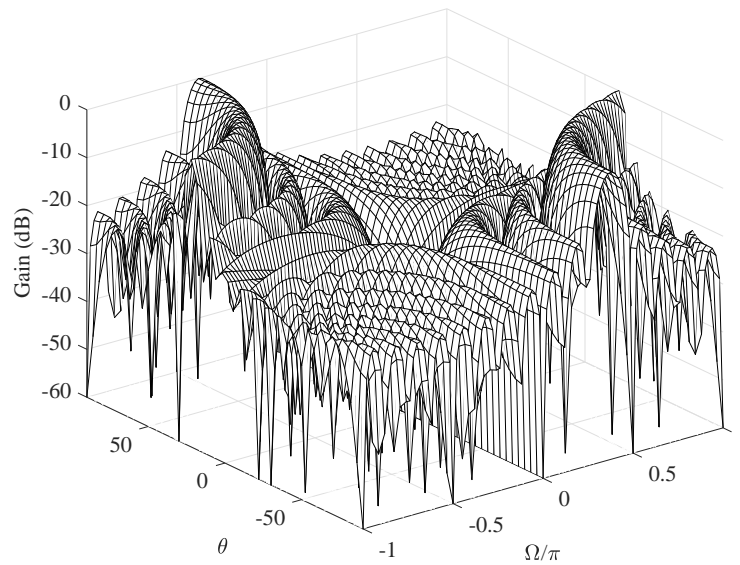
The simulations here are based on a 16-sensor ( $M = 16$ ) ULA and the desired signal arrives from the broadside ( $\theta_d = 0$ ). The received signals are processed by the  $16 \times 16$  DFT-based transformation matrix and pass through the highpass filters. We have assumed that the highpass filters have an ideal brick-wall shape response and to have a close approximation, linear-phase 101-tap FIR filters with a common delay of 50 samples are employed. The beam pattern of a sample row vector with respect to signal frequency  $\Omega$  and DOA angle  $\theta$  before and after highpass filtering is shown in Fig. 5.

1) *Effect on noise and directional signals:* To see the effect of the whole system on noise, we generate spatially and temporally white noise at the array sensors with unit power. The power spectrum density of noise before and after the proposed noise reduction process is shown in Fig. 6a and Fig. 6b, respectively. It can be seen that the noise power has been reduced significantly at lower frequencies, while for higher frequencies, the reduction becomes less and less. Overall the power of noise has been reduced clearly.

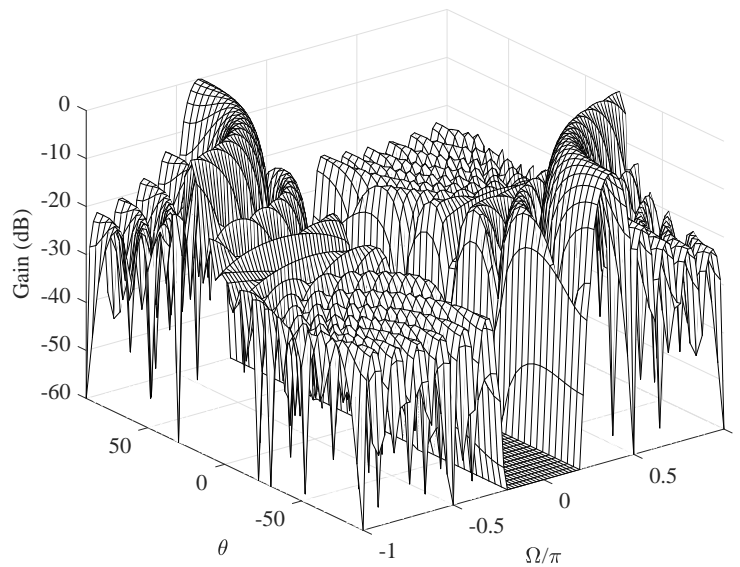
For the received directional signals, as discussed there should not be any change after the proposed processing in the ideal case. However, the response of the row vectors of the transformation is not ideal and as a result, a small amount of the



(a) 2D beam pattern of a sample row vector.

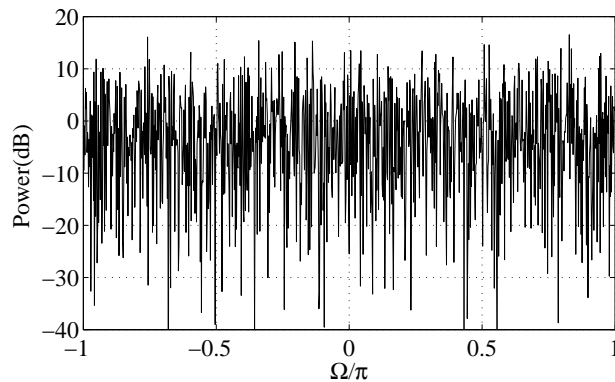


(b) 3D beam pattern of the row vector shown in Fig. 5a before highpass filtering.

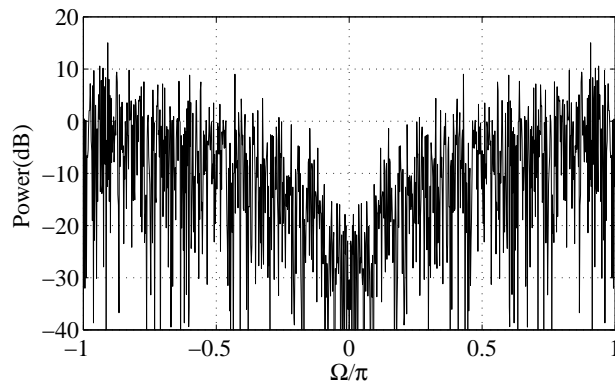


(c) 3D beam pattern of the row vector shown in Fig. 5a after highpass filtering.

Figure 5: The beam pattern of a sample row vector before and after highpass filtering (ULA,  $M=16$ ).



(a) Power spectrum density of noise before processing.



(b) Power spectrum density after processing.

Figure 6: The power spectrum density of the spatially and temporally white noise before and after processing ( $M=16$ ).

directional signals will exist at the lower sidelobe region and it will be removed by the following high pass filters. To show this effect, a wideband signal with unit power is applied to the array from the broadside, and both the mean square error (MSE) between the original one and the one after the proposed processing and the output power  $P_o$  to the input power  $P_i$  ratio are calculated. The results for different array size ( $M$ ) are shown in Table I, where it can be seen that the effect on the directional signal can be ignored for  $M \geq 16$ . We also calculated the same results for the unit power white noise and they are shown in Table II. It can be seen that the power ratio is getting closer to the ideal case of -3dB as we increase  $M$ .

$M$	MSE	$P_o/P_i$ (dB)
10	0.0339	-0.15
16	0.0205	-0.09
20	0.0114	-0.05
30	0.0069	-0.03
40	0.0023	-0.01

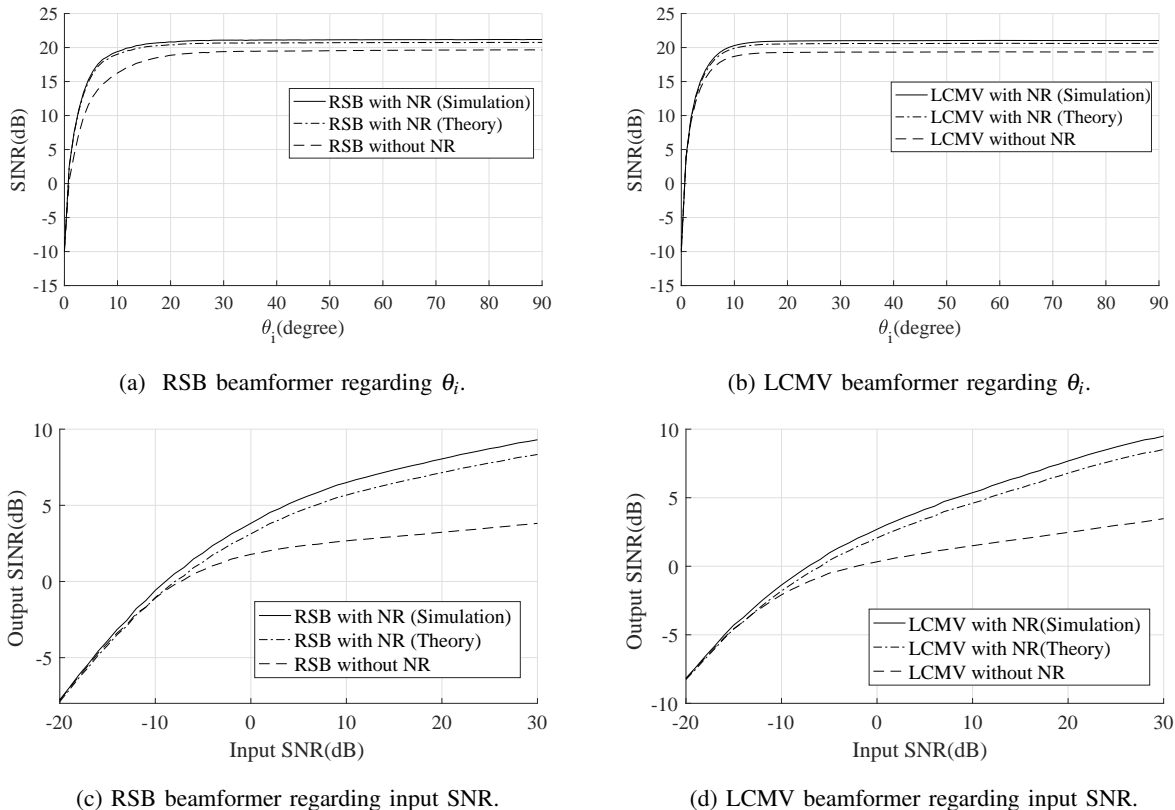
Table I: MSE and power loss for the directional signal.

2) *Effect on beamforming performance:* Now we examine the effect of the proposed method on the performance of both the RSB beamformer and the LCMV beamformer.

A desired bandlimited wideband signal with bandwidth of  $[0.3\pi : \pi]$  is received by the  $M = 16$  array sensors from the broadside. An interfering signal with the same bandwidth and a -10dB SIR arrives with a varying DOA angle. The received

$M$	MSE	$P_{no}/P_{ni}$ (dB)	ideal $P_{no}/P_{ni}$ (dB)
10	0.3988	-2.21	-2.26
16	0.4259	-2.41	-2.53
20	0.4301	-2.52	-2.62
30	0.4487	-2.65	-2.74
40	0.4637	-2.79	-2.80

Table II: MSE and power loss for white noise.

Figure 7: SINR performance of both beamformers with and without the proposed noise reduction (NR) method ( $M=16, J=100$ ).

array signals are processed by the proposed noise reduction method and then the recovered array signals with an increased SNR are used as input to the beamformer. The input SNR is 0dB and the TDL length  $J = 100$ .

The output SINR performances of both beamformers with and without the proposed preprocessing are compared in Fig. 7a and Fig. 7b as a function of the DOA angle of the interfering signal  $\theta_i$ , where the theoretical value is based on the result derived in Sec. IV. We can see that the simulation result matches the theoretical one very well. With the change of the direction of the interfering signal, except for the region where DOA of the interfering signal is very close to the desired signal, an almost constant improvement of about 2dB can be observed.

It is also important to analyse how the SINR performance of the proposed method varies with different input SNRs. Seven interfering signals are applied to the system, each with a -10dB input SIR, and their DOAs are  $\theta_i = 10^\circ, 20^\circ, 30^\circ, 40^\circ, 50^\circ, 60^\circ$  and  $70^\circ$ , respectively. All the other settings are the same as before. The results are shown in Fig. 7c and Fig. 7d. As expected, a higher output SINR has been achieved by the proposed method for both beamformers especially when the input SNR is larger than -10dB and generally the improvement becomes larger when input SNR increases.



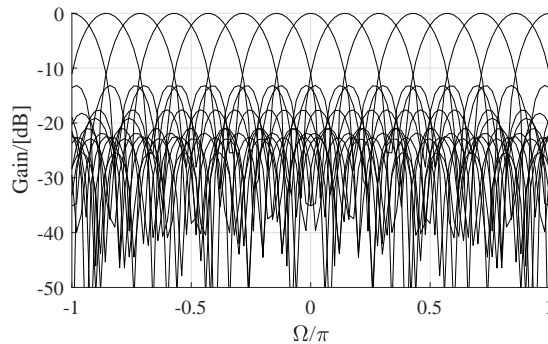


Figure 8: Frequency response of the row vectors of the  $15 \times 15$  designed transformation matrix for NLAs.

### B. Performance of NR method for NLA

These simulations are based on an  $M = 15$  NLA example provided in [30], with the sensor locations listed in Table III, where  $\lambda$  is the wavelength associated with the normalized frequency  $\Omega = \pi$ . The  $15 \times 15$  transformation matrix is obtained by the design procedure described in Sec. V, and its frequency response is shown in Fig. 8. The other settings are the same as in the ULA case.

n	$d_n/\lambda$	n	$d_n/\lambda$	n	$d_n/\lambda$
1	0	6	4.09	11	6.72
2	0.81	7	4.24	12	7.58
3	1.62	8	5.00	13	8.38
4	2.42	9	5.81	14	9.19
5	3.28	10	5.96	15	10

Table III: Sensor locations for the wideband NLA example.

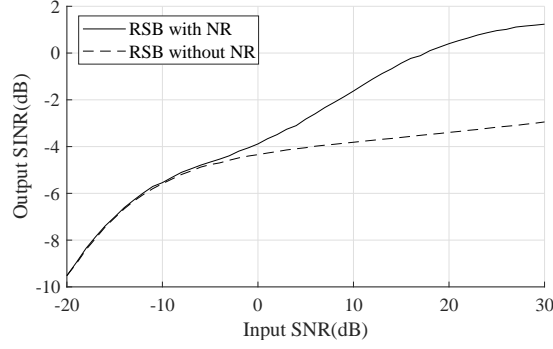
The results are shown in Fig. 9, and we can see that a higher output SINR is achieved by the proposed method for both beamformers, especially when the input SNR is larger than 0dB and generally the improvement becomes larger when input SNR increases. However, compared to the ULA case, for input SNR smaller than 0 dB, there is not as much improvement. After checking the designed transformation matrix, we found that it is far away from being unitary and has a large condition number, which could be the reason for such a behavior. As mentioned at the end of Sec. V, further research is needed for designing a unitary transformation matrix for NLAs with the desired frequency responses.

### C. Discussion

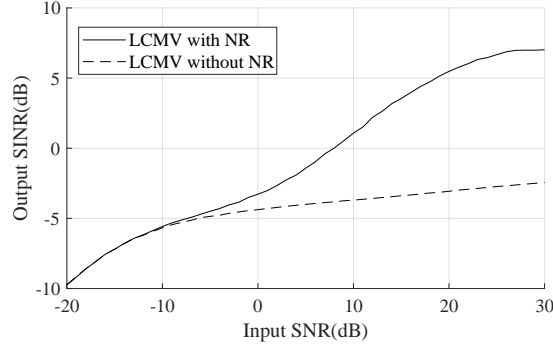
As can be seen from the proposed structure, we do not need any prior information about the impinging signals to reduce the noise level and increase the overall SNR by about 3dB. However, although the SNR has been improved, the noise is not white any more, as specified in (28), whose effect on the ultimate performance of the system can not be seen directly. That is why we have provided both theoretical analyses and computer simulations to show that indeed by the proposed method, the performance of the two studied beamformers has been improved.

The above result is obtained from the viewpoint of reducing the noise level of the received signals.

Actually by studying the structure further, it is realised that the proposed structure is equivalent to a traditional TDL system, but the length of TDL is much larger. As a result, if we apply the same LCMV beamformer (with the same TDL length)



(a) RSB beamformer.



(b) LCMV beamformer.

Figure 9: SINR performance of both beamformers with and without the proposed noise reduction method for the NLA.

to both the original set of array signals and the new set of array signals after the proposed preprocessing, the latter one will be equivalent to a kind of LCMV beamformer but with much longer TDLs, and hence the improved performance. From this viewpoint, the proposed method can also be considered as a low-complexity approach to adaptive beamforming. Certainly another advantage is that the proposed preprocessing is standard and can be applied to the original array signals, whatever the following processing (either beamforming or DOA estimation, or tracking, etc.) is. As shown in our study for DOA estimation based on the proposed structure in [13], the improved SNR can be translated into improved DOA estimation performance too.

To show that the overall combination of the proposed noise reduction part and the following TDL-based beamformer is equivalent to a new beamformer with a much longer TDL, i.e., the noise reduction method alongside the TDL attached can be modelled as an equivalent TDL with a larger length, we first derive the following result:

$$y[n] = \sum_{k=0}^{M-1} \sum_{n_0=0}^{l_{hp}+J-2} x_k[n-n_0] \sum_{p=0}^{M-1} a_{pk} \sum_{m=0}^{M-1} \tilde{a}_{mp} \sum_{j=0}^{J-1} w_{mj} h_p[n_0-j], \quad (59)$$

where  $l_{hp}$  is the length of the highpass filters and  $[\mathbf{A}^{-1}]_{mp} = \tilde{a}_{mp}$ .

By arranging (59), we have:

$$y[n] = \sum_{k=0}^{M-1} \sum_{n_0=0}^{l_{hp}+J-2} \sum_{p=0}^{M-1} \sum_{m=0}^{M-1} \sum_{j=0}^{J-1} a_{pk} \tilde{a}_{mp} w_{mj} h_p[n_0-j] x_k[n-n_0]. \quad (60)$$

By assuming  $\tilde{w}_{k,n_0} = \sum_{p=0}^{M-1} \sum_{m=0}^{M-1} \sum_{j=0}^{J-1} a_{pk} \tilde{a}_{mp} w_{mj} h_p[n_0-j]$ , (59) becomes

$$y[n] = \sum_{k=0}^{M-1} \sum_{n_0=0}^{l_{hp}+J-2} \tilde{w}_{k,n_0} x_k[n-n_0], \quad (61)$$

which is the equivalent TDL of a length  $J_{eq} = l_{hp} + J - 1$  for the noise reduction method combined with a TDL of length  $J$ .

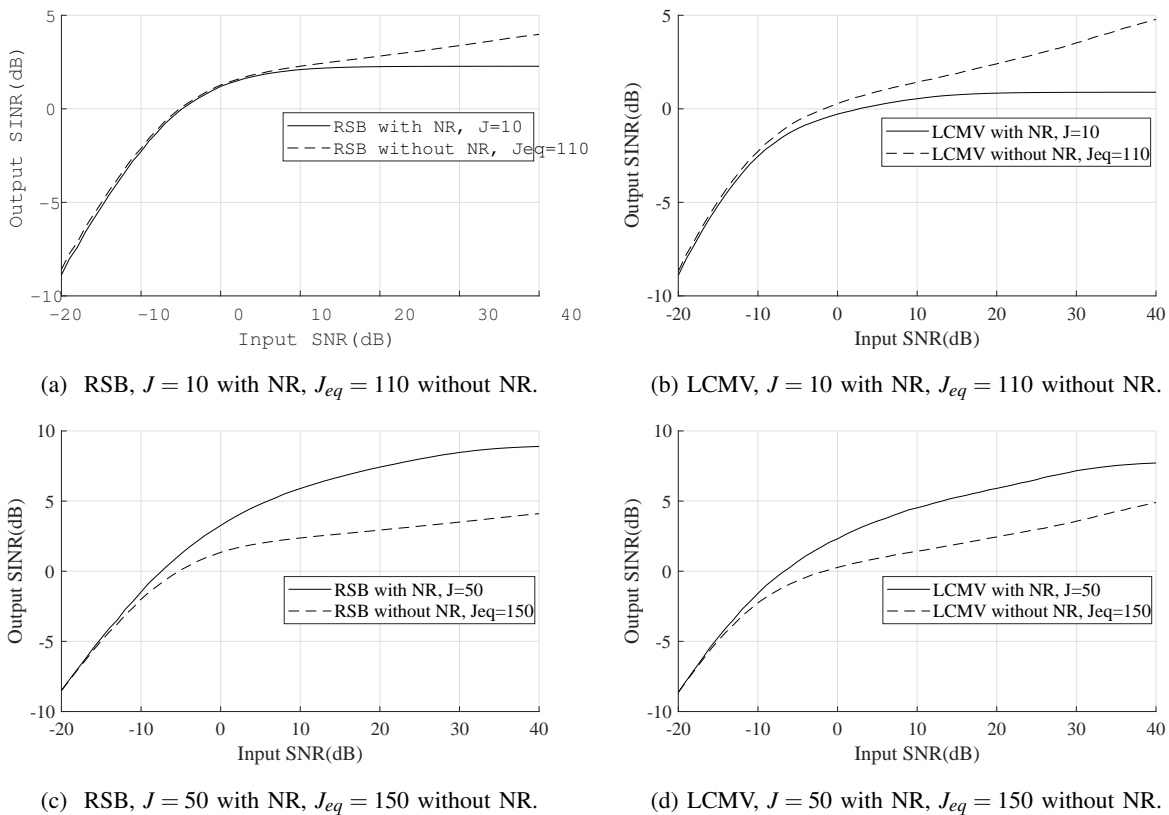


Figure 10: SINR performance of both beamformers with NR method and without NR with equivalent length,  $l_{hp} = 101$ .

The question here is, since the noise reduction method can be modeled as a TDL, which one of the following gives us a better performance: using the noise reduction method and a TDL with length  $J$  or using a larger TDL with length  $J_{eq} = l_{hp} + J - 1$ . We may think the latter one will give a better performance, although it may have the highest implementation complexity, since a globally optimum solution can be found without constraints imposed by the proposed specific noise reduction process. However, the real picture is much complicated, due to numerical issues involved in calculating the optimum beamforming coefficients based on inversion of correlation matrices of difference sizes. The longer the TDL, the larger the dimension of the matrix involved and the more likely it will cause additional errors in performing matrix inversion.

To show this, again we consider the two types of TDL-based beamformers, i.e., the RSB and the LCMV beamformers. The SINR performance of both beamformers with the noise reduction method and without the method with the equivalent length  $J_{eq}$  is shown in Fig. 10. All the simulation conditions are the same as in Section VI-A. When the length of the beamformer is short ( $J=10$  and equivalent of  $J_{eq}=110$ ) as in Fig. 10a and Fig. 10b, the performance of the beamformers without preprocessing is better, as expected in theory. When the length of the beamformers is larger ( $J=50$  and equivalent of  $J_{eq}=150$ ) as in Fig. 10c and Fig. 10d, the performance of the beamformers with preprocessing is better.

A direct advantage of the proposed noise reduction preprocessing is in reducing the computational complexity of the beamformers. The computational complexity of the proposed noise reduction method (including the beamforming part), the directly implemented RSB and LCMV beamformers is presented in Table IV, where  $N$  is the number of signal samples at each sensor. As  $J \ll J_{eq}$ , the complexity with the proposed method is much smaller than the direct implementation case.

Algorithm	without NR	with NR
RSB	$\mathcal{O}(M^3 J_{eq}^3) + M^2 J_{eq}^2 N + M^2 J_{eq}^2 + M J_{eq} N$	$\mathcal{O}(M^3 J^3) + M^2 J^2 N + M^2 J^2 + M J N + 2M^2 N + M I_{hp}^2 + M N I_{hp}$
LCMV	$\mathcal{O}(M^3 J_{eq}^3) + \mathcal{O}(J_{eq}^3) + 2M^2 J_{eq}^3 + 2M J_{eq}^3 + M^2 J_{eq}^2 N + M J_{eq}^2$	$\mathcal{O}(M^3 J^3) + \mathcal{O}(J^3) + 2M^2 J^3 + 2M J^3 + M^2 J^2 N + M J^2$ $+ 2M^2 N + M I_{hp}^2 + M N I_{hp}$

Table IV: Computational complexity of the noise reduction based implementation, the RSB and LCMV beamformers.

## VII. CONCLUSION

A method for mitigating the effect of white noise without affecting the directional signals in wideband arbitrary linear arrays has been introduced. With the proposed method, a maximum 3dB improvement in total signal power to total noise power ratio (TSNR) can be achieved in the ideal case. A detailed study of the proposed method has been performed and the effect of the method on the spectra of both the directional signals and in particular white noise is analysed. The increased TSNR can be translated into performance improvement in various array signal processing applications and as an example, its effect on beamforming is investigated in detail based on two representative beamformers: the RSB and the LCMV beamformers. As demonstrated by both theoretical analysis and simulation results, a clear improvement in performance in terms of output SINR has been achieved.

## REFERENCES

- [1] H. L. Van Trees, *Optimum Array Processing, Part IV of Detection, Estimation, and Modulation Theory*. New York: Wiley, 2002.
- [2] W. Liu and S. Weiss, *Wideband Beamforming: Concepts and Techniques*. Chichester, UK: John Wiley & Sons, 2010.
- [3] D. Feng, M. Bao, Z. Ye, L. Guan, and X. Li, "A novel wideband DOA estimator based on Khatri–Rao subspace approach," *Signal Processing*, vol. 91, no. 10, pp. 2415–2419, April 2011.
- [4] Z. M. Liu, Z. T. Huang, and Y. Y. Zhou, "Direction-of-arrival estimation of wideband signals via covariance matrix sparse representation," *IEEE Transactions on Signal Processing*, vol. 59, no. 9, pp. 4256–4270, Sep. 2011.
- [5] Y. D. Zhang, M. G. Amin, F. Ahmad, and B. Himed, "DOA estimation using a sparse uniform linear array with two CW signals of co-prime frequencies," in *Proc. IEEE International Workshop on Computational Advances in Multi-Sensor Adaptive Processing*, Saint Martin, December 2013, pp. 404–407.
- [6] J. A. Luo, X. P. Zhang, and Z. Wang, "A new subband information fusion method for wideband DOA estimation using sparse signal representation," in *Proc. IEEE International Conference on Acoustics, Speech, and Signal Processing*, Vancouver, Canada, May 2013, pp. 4016–4020.
- [7] J. Y. Lee, R. E. Hudson, and K. Yao, "Acoustic DOA estimation: An approximate maximum likelihood approach," *IEEE Systems Journal*, vol. 8, no. 1, pp. 131–141, Mar. 2014.
- [8] Y.-S. Yoon, L. M. Kaplan, and J. H. McClellan, "TOPS: new DOA estimator for wideband signals," *IEEE Transactions on Signal Processing*, vol. 54, no. 6, pp. 1977–1989, June 2006.
- [9] Q. Shen, W. Liu, W. Cui, S. L. Wu, Y. D. Zhang, and M. Amin, "Low-complexity direction-of-arrival estimation based on wideband co-prime arrays," *IEEE Trans. Audio, Speech and Language Processing*, vol. 23, pp. 1445–1456, September 2015.
- [10] B. Widrow, J. R. Glover, J. M. McCool, J. Kaunitz, C. S. Williams, R. H. Hearn, J. R. Zeidler, J. E. Dong, and R. C. Goodlin, "Adaptive noise cancelling: Principles and applications," *Proceedings of the IEEE*, vol. 63, no. 12, pp. 1692–1716, 1975.
- [11] T. B. Spalt, C. R. Fuller, T. F. Brooks, and W. Humphreys, "A background noise reduction technique using adaptive noise cancellation for microphone arrays," in *17th AIAA/CEAS Aeroacoustics Conference, American Institute of Aeronautics and Astronautics, Portland, OR*, 2011, pp. 2715–2731.
- [12] W. Liu and R. J. Langley, "An adaptive wideband beamforming structure with combined subband decomposition," *IEEE Transactions on Antennas and Propagation*, vol. 89, pp. 913–920, July 2009.
- [13] M. R. Anbiyai, W. Liu, and D. C. McLernon, "Performance improvement for wideband DOA estimation with white noise reduction based on uniform linear arrays," in *Proc. IEEE, Sensor Array and Multichannel Signal Processing Workshop (SAM)*, Rio de Janeiro, Brazil, July 2016.
- [14] R. T. Compton, Jr., "The relationship between tapped delay-line and FFT processing in adaptive arrays," *IEEE Transactions on Antennas and Propagation*, vol. 36, no. 1, pp. 15–26, January 1988.
- [15] R. T. Compton, "The bandwidth performance of a two-element adaptive array with tapped delay-line processing," *IEEE Transactions on Antennas and Propagation*, vol. 36, no. 1, pp. 4–14, January 1988.
- [16] F. W. Vook and R. T. Compton, Jr., "Bandwidth performance of linear adaptive arrays with tapped delay-line processing," *IEEE Transactions on Aerospace and Electronic Systems*, vol. 28, no. 3, pp. 901–908, July 1992.

- [17] N. Lin, W. Liu, and R. J. Langley, "Performance analysis of an adaptive broadband beamformer based on a two-element linear array with sensor delay-line processing," *Signal Processing*, vol. 90, pp. 269–281, January 2010.
- [18] O. L. Frost, III, "An algorithm for linearly constrained adaptive array processing," *Proceedings of the IEEE*, vol. 60, no. 8, pp. 926–935, August 1972.
- [19] A. Jakobsson, S. R. Alty, and S. Lambouharan, "On the implementation of the linearly constrained minimum variance beamformer," *IEEE Transactions on Circuits & Systems II: Express Briefs*, vol. 53, no. 10, pp. 1059–1062, October 2006.
- [20] W. Liu, S. Weiss, and L. Hanzo, "A subband-selective broadband GSC with cosine-modulated blocking matrix," *IEEE Transactions on Antennas and Propagation*, vol. 52, pp. 813–820, March 2004.
- [21] K. Takao and K. Uchida, "Beamspace partially adaptive antenna," *IEE Proceedings H, Microwaves, Antennas and Propagation*, vol. 136, pp. 439–444, December 1989.
- [22] T. Sekiguchi and Y. Karasawa, "Wideband beamspace adaptive array utilizing FIR fan filters for multibeam forming," *IEEE Transactions on Signal Processing*, vol. 48, no. 1, pp. 277–284, January 2000.
- [23] W. Liu, R. Wu, and R. Langley, "Design and analysis of broadband beamspace adaptive arrays," *IEEE Transactions on Antennas and Propagation*, vol. 55, no. 12, pp. 3413–3420, December 2007.
- [24] B. Mulgrew, P. Grant, and J. Thompson, "Random signal analysis," in *Digital Signal Processing*. Macmillan Education UK, 1999, pp. 176–205.
- [25] R. Bracewell and P. B. Kahn, "The Fourier transform and its applications," *American Journal of Physics*, vol. 34, no. 8, pp. 712–712, 1966.
- [26] F. Vook and R. Compton Jr, "Bandwidth performance of linear adaptive arrays with tapped delay-line processing," *IEEE Transactions on Aerospace and Electronic Systems*, vol. 28, no. 3, pp. 901–908, 1992.
- [27] O. L. Frost III, "An algorithm for linearly constrained adaptive array processing," *Proceedings of the IEEE*, vol. 60, no. 8, pp. 926–935, 1972.
- [28] Y. Zhao, W. Liu, and R. J. Langley, "An application of the least squares approach to fixed beamformer design with frequency invariant constraints," *IET Signal Processing*, pp. 281–291, June 2011.
- [29] B. D. Carlson, "Covariance matrix estimation errors and diagonal loading in adaptive arrays," *IEEE Transactions on Aerospace and Electronic Systems*, vol. 24, pp. 397–401, July 1988.
- [30] M. B. Hawes and W. Liu, "Sparse microphone array design for wideband beamforming," in *Proc. International Conference on Digital Signal Processing*, Santorini, Greece, July 2013.